ELSEVIER

Carbohydrate Research 312 (1998) 123–129

CARBOHYDRATE RESEARCH

Assignment of non-crystalline forms in cellulose I by CP/MAS ^{13}C NMR spectroscopy

Kristina Wickholm, Per Tomas Larsson*, Tommy Iversen

Swedish Pulp and Paper Research Institute, STFI, Box 5604, SE-114 86, Stockholm, Sweden

Received 8 June 1998; accepted 27 July 1998

Abstract

Non-crystalline forms of cellulose in birch pulp, cotton linters and *Cladophora* sp were studied by CP/MAS ^{13}C NMR spectroscopy. New assignments were made for the NMR-signals in the lower shift part of the C-4 region (80–86 ppm). These signals were assigned to cellulose at accessible fibril surfaces, cellulose at inaccessible fibril surfaces and hemicellulose. Also, further evidence was found for para-crystalline cellulose as an ''in-fibril'' form, inaccessible to the surrounding solvent.

Keywords: Cellulose; NMR; Hydrolysis; Chemometrics; Fibril surfaces; ^{13}C T_1-Relaxation time

1. Introduction

In native cellulose fibers of the cellulose I type, cellulose chains are aggregated to form fibrils that are deposited in the cell wall during biosynthesis. Since technologically important physical properties of cellulose fibers, and their behavior in chemical reactions, are related to the super-molecular structure of the fiber polymers, the molecular ordering has interested researchers for many years. It is generally assumed that in these fibrils ordered regions alternate with less ordered regions (for recent reviews see Krässig [1] and Hon [2]). In previous papers [3,4], we reported a method for quantifying the states of order found within cellulose I, based on CP/MAS ^{13}C NMR in combination with spectral fitting. The most informative region in a NMR spectrum of cellulose I is a signal cluster with a distribution between 80 and 92 ppm. This region contains fairly sharp signals corresponding to C-4 carbons situated in crystalline cellulose Iα and Iβ domains together with para-crystalline cellulose [4]. The C-4 carbons of more disordered regions are distributed in a broad band ranging from 80 to 86 ppm [3–8]. In a recent article, Newman [9] used NMR-spectroscopy to investigate the molecular ordering in cellulose I. In the disordered region, a pair of signals at 83.9 and 85.0 ppm was assigned to two non-equivalent sites at the crystallite surfaces. (The offset of about 0.7 ppm, between the assignments reported here and those of Newman [9], is probably due to the different external standards used for calibrating the chemical shift scale with respect to TMS.)

The aim of this study was to investigate the effects of acid hydrolysis and solvent exchange on the spectral features of different cellulose substrates, with emphasis on the clarification of the super-molecular origin of the non-crystalline cellulose I

* Corresponding author. Tel.: +46-8-676-7000; fax: +46-8-411-5518.

0008-6215/98/$—see front matter
PII S0008-6215(98)00236-5

forms. Bleached birch kraft pulp and cotton linters were chosen as representatives for plant celluloses. Experiments on an well-ordered algal cellulose isolated from *Cladophora* sp. was included to examine more thoroughly the presence of any cellulose Iα to Iβ allomorph transformation [10].

2. Results

The NMR spectra of the starting materials are shown in Fig. 1. The NMR spectra from the hydrolysis series are compiled in a PCA score plot shown in Fig. 2. The directions indicated by the orthogonal arrows shown in the figure mainly represent cellulose Iα/Iβ allomorph composition (PC1′) and cotton linters/birch pulp group separation (PC2′). The common projection of the birch pulp and cotton linters objects onto PC1′ is due to their similar cellulose Iα content (2–8% in all samples, data not shown). No detectable cellulose Iα to cellulose Iβ allomorph interconversion was detected in the *Cladophora* cellulose (51% cellulose Iα and 29% cellulose Iβ [4]) under these experimental conditions [10,11]. The ordering with respect to hydrolysis time observed along PC2′ gives no interpretable information concerning the events occurring during the hydrolysis. Such information is probably hidden by the differences between the two sample types.

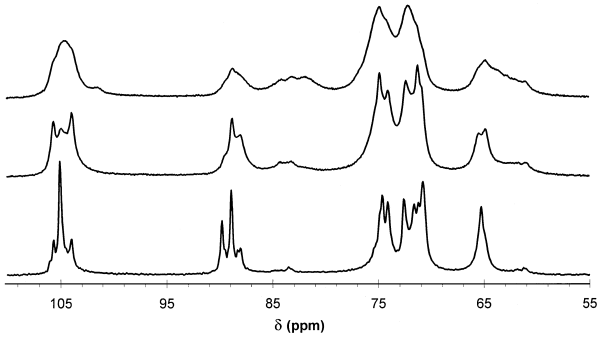

Fig. 1. CP/MAS ^{13}C NMR spectra of, from bottom to top, *Cladophora* cellulose, cotton linters and birch pulp.

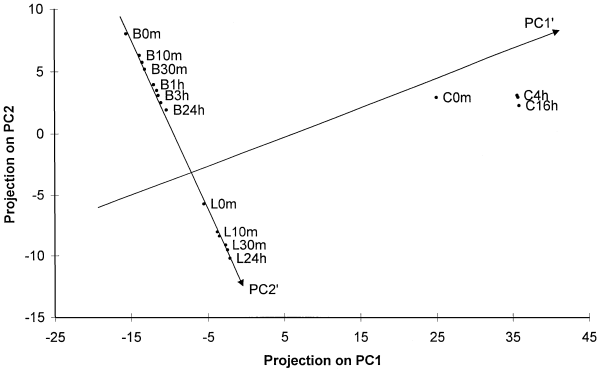

Fig. 2. PCA score plot of the objects (NMR spectra) projected onto the first two of the retained principal components, PC1 and PC2. On some of the points, labels are shown. B represents birch pulp, C represents *Cladophora* cellulose and L represents cotton linters. The numbers in the labels are hydrolysis time in either minutes (m) or hours (h). The solid arrows shown are the rotated principal components PC1′ and PC2′ constructed in order to obtain information concerning the chemically most significant directions in the plot.

Based on the results in Fig. 2, spectral fitting [4] was performed on the C-4 region of the birch pulp spectra from the hydrolysis series. One spectral fitting result is shown in Fig. 3 and in Table 1, and the pooled results from all the spectra are shown in Fig. 4, where it is apparent that, even after a prolonged hydrolysis of the birch pulp, the broad signal at 83.4 ppm could not be completely removed, indicating that this fitted spectral line contains contributions from several different components. In Table 2, the results of a sugar analysis and of limiting viscosity number and yield determinations on the birch pulp at different stages during the hydrolysis are shown.

The result from an experiment in which water in hydrolysed cotton linters was replaced by methanol is shown in Fig. 5. The effect of the replacement dominates in the spectral region assigned to fibril surfaces. The ^{13}C T_1-relaxation time (spin-lattice) data for the C-4 region of hydrolysed cotton linters are compiled in Table 3 and they show significant differences between the different cellulose forms. The relaxation times of the crystalline celluloses Iα and Iβ were too long to be determined by the delay times used in the experiment.

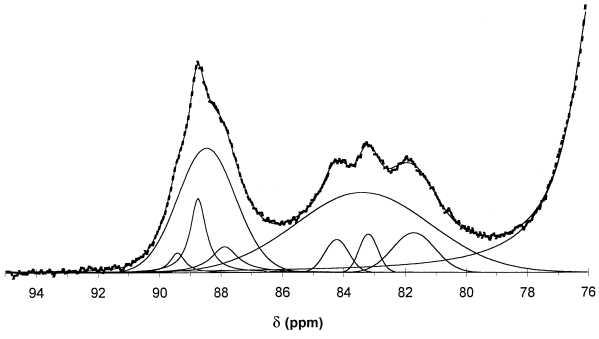

Fig. 3. The fitting of the C-4 spectral region of a birch pulp hydrolysed for 10 min. The dotted line represents the experimental spectrum. The fitted spectral lines and their superposition are shown as solid lines. The results of the fitting and the assignments are compiled into Table 1.

Table 1
Assignments of signals in the C-4 region of a birch pulp spectrum

Assignment	Chemical shift (ppm)	FWHH[a] (Hz)	Relative intensity (%)
Iα	89.42 (0.03)[b]	44 (11)	1.8 (0.8)
I($\alpha+\beta$)	88.74 (0.01)	46 (4)	7.1 (1.2)
Para-crystalline	88.45 (0.10)	168 (9)	29.9 (3.2)
Iβ	87.87 (0.04)	81 (17)	4.3 (1.9)
Accessible fibril surfaces	84.22 (0.05)	70 (16)	3.2 (1.1)
Inaccessible fibril surfaces and xylan	83.38 (0.20)	388 (44)	43.9 (3.1)
Accessible fibril surfaces	83.18 (0.03)	53 (8)	2.9 (0.6)
Xylan	81.72 (0.11)	121 (22)	6.8 (2.1)

The birch pulp was subjected to hydrolysis for 10 min.
[a]FWHH is the full width at half-height.
[b]Values in parentheses are the standard errors.

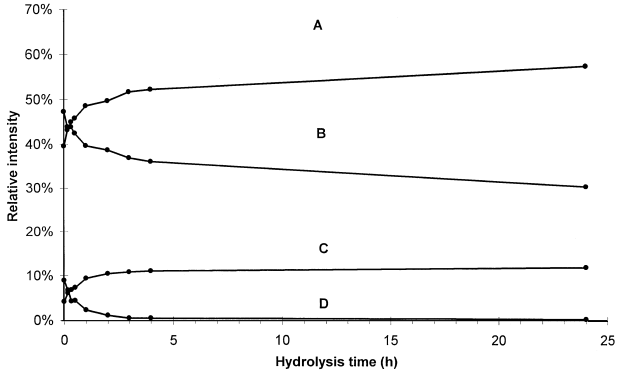

Fig. 4. The pooled relative signal intensities obtained by spectral fitting of the C-4 region of birch pulp spectra, at different stages of the hydrolysis series. (A) Crystalline Iα and Iβ and para-crystalline cellulose (sum of signal intensities at 89.4, 88.7, 88.5 and 87.9 ppm). (B) At short hydrolysis times, a mixture of cellulose at inaccessible fibril surfaces and xylan that becomes progressively depleted in xylan as the hydrolysis proceeds (signal intensity at 83.4 ppm). (C) Cellulose at accessible fibril surfaces (sum of signal intensities at 84.2 and 83.2 ppm). (D) Xylan (signal intensity at 81.7 ppm).

The spectral C-4 region from a long-time acquisition performed on *Cladophora* cellulose is shown in Fig. 6. A significant difference in intensity is observed between the two signals assigned to fibril surfaces.

3. Discussion

Fig. 3 shows the spectral fitting of the C-4 region of a birch pulp spectrum. The region typical of the less ordered carbohydrate forms (80–86 ppm) contains several signals that have not yet been assigned to distinct cellulose forms. It has been suggested that the two signals at 83.2 and 84.2 ppm originate from cellulose at fibril (or "crystallite") surfaces [8,9], that the wide signal at 83.4 ppm originates from amorphous cellulose, and that the signal at

Table 2
Characteristics of the samples at different stages during the hydrolysis

Sample	Hydrolysis time	Xylose content (%)	Yield (%)	Limiting viscosity number (dm^3/kg)
Birch pulp	0	26		710
	10 min	16		
	20 min	12		
	30 min	12	80	150
	1 h	6		
	2 h	3		
	3 h	2		
	4 h	2	65	120
	24 h	1		
Cotton linters	0			420
	10 min			
	20 min			
	30 min		93	100
	4 h		87	100
	24 h			
Cladophora cellulose	0			> 2000
	30 min		83	1290
	4 h		80	800
	16 h			

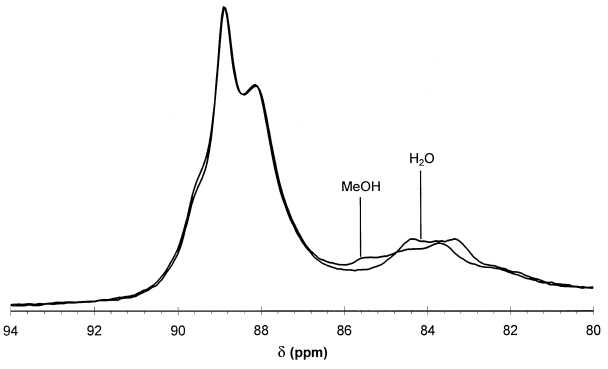

Fig. 5. The C-4 regions of cotton linters for a sample with and without replacement of water by methanol. The spectrum of the cotton linters soaked in methanol shows the largest deviations from the spectrum of the cotton linters soaked in water in the spectral region typical for the unordered forms of cellulose (80–86 ppm). The spectral region typical for the ordered form of cellulose (86–92 ppm) remains comparatively intact.

Table 3
The ^{13}C spin-lattice relaxation times as obtained from spectral fitting of the C-4 region of cotton linters

Cellulose form	Chemical shift (ppm)	^{13}C T_1 (s)
Para-crystalline	88.4	138 (80)[a,b]
Inaccessible fibril surfaces	83.8	38.8 (7.0)
Accessible fibril surface	84.3	18.5 (3.6)
Accessible fibril surface	83.4	11.1 (1.4)

The values quoted are averages of two measurements.
[a]The values in parentheses are the standard errors.
[b]The large uncertainty in the relaxation time for the para-crystalline cellulose is due to the limited maximum decay time used (40 s).

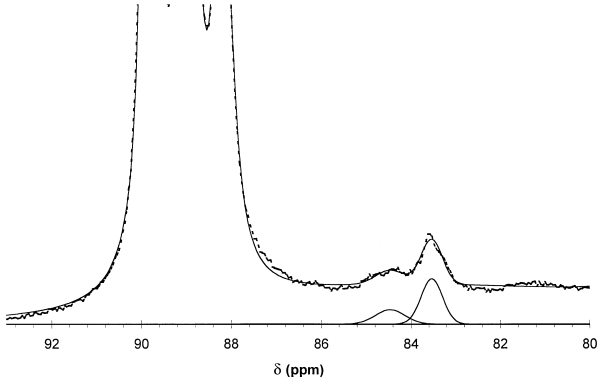

Fig. 6. The enlarged C-4 region from a long-time acquisition performed on a *Cladophora* cellulose sample. The figure shows only the lines fitted to the signals originating from the cellulose at accessible fibril surfaces.

81.7 ppm originates from less ordered forms of carbohydrates, e.g., hemicellulose and cellulose oligomers [4].

The results of the experiment in which water in cotton linters was replaced by methanol, shown in Fig. 5, and the relaxation times in Table 3 do indeed support the interpretation of the signals at 84.2 and 83.2 ppm as cellulose at fibril surfaces. The short relaxation times indicate a high degree of mobility consistent with a cellulose form accessible to a surrounding solvent. Hence, the suggested interpretation (cellulose at fibril surfaces [8,9]) is sharpened to cellulose at accessible fibril surfaces. Further, the lack of substantial change due to solvent exchange in the spectral region typical of ordered forms of cellulose (86–91 ppm) and the comparatively long relaxation time of the para-crystalline cellulose support the interpretation that the para-crystalline form is an "in-core" or "in-fibril" form inaccessible to the surrounding solvent.

It is evident in Fig. 4 that the broad signal at 83.4 ppm (previously assigned to amorphous cellulose) contains contributions from more than one form of carbohydrate. This is seen from the levelling-off of the pooled relative signal intensity, reached after 4–5 h of hydrolysis. The loss of signal intensity at 24 h of hydrolysis from the signals at 83.4 and 81.7 ppm (26%) compares favorably with the results of the sugar analysis (25% loss of xylose) shown in Table 2. Hence, the initial phase seen in Fig. 4 corresponds mainly to the removal of xylan from the birch pulp. The resistance towards hydrolysis, the position in the spectrum, the line width and the relaxation time of the signal intensity remaining at 83.4 ppm at long hydrolysis times, suggest that it represents some form of cellulose surface structure inaccessible to solvents and to the effects of hydrolysis.

If the fibrillar form of cellulose I is taken into consideration, the observed effects can be accounted for if the cellulose (after 5 h or more of hydrolysis) is considered to consist of aggregates of coaxial fibrils with abundant fibril-to-fibril contact surfaces. (Any solvent inaccessible surfaces inside the fibril may also contribute to this signal intensity, although this type of surface appears not to dominate, *vide infra*). Such fibril-to-fibril contact surfaces offer a coherent explanation of the experimental findings. The position in the spectrum of such a cellulose form would be similar to that of the accessible surfaces. The large variability in hydrogen bonding pattern (hydrogen bonding either between fibrils or between neighbouring hydroxyl groups on the same fibril surface) at these surfaces accounts for a large line width. A ^{13}C T_1-relaxation time longer than that of the solvent-exposed accessible surfaces would also be reasonable to expect, and finally the cellulose at the fibril-to-fibril contact surfaces would be inaccessible given a short contact distance.

According to the sugar analysis about 1% of xylose remains at the longest hydrolysis time (24 h), indicating the presence of some xylan associated to solvent inaccessible fibril surfaces. The interpretation of the signal intensity at 83.4 ppm, remaining after prolonged hydrolysis, as signal from inaccessible fibril surfaces can be tested, since all signal intensity originating from fibril surfaces (accessible and inaccessible) is accounted for if the interpretation is correct. Given that the cellulose spectrum is quantitative [4], the lateral fibril dimensions can be determined from the signal intensities of the C-4

region of the spectrum, once a suitable model for the form of the fibril cross-section is given. A simple model consists of a fibril with a square cross-section, and the fraction of the signal intensity from cellulose at fibril surfaces (q) for this model is given by the equation:

$$q = \frac{4n - 4}{n^2} \quad (1)$$

Where n is the number of cellulose polymers perpendicular to the cross-section along one side of the square fibril cross-section. A conversion factor of 0.55 nm per cellulose polymer [1] has been used to calculate the results shown in Table 4. The agreement with previous fibril width determinations for similar types of cellulose is good, supporting the interpretation of the hydrolysis resistant signal at 83.4 ppm as being related to inaccessible fibril-to-fibril contact surfaces. (A dominance of internal fibril surfaces would corrupt the lateral fibril dimensions estimates from NMR as compared to those obtained by microscopy methods.) A word of caution is appropriate. The calculation of lateral fibril dimensions can only be performed on hydrolysed samples since it is necessary to remove the interfering signals from hemicelluloses (e.g., xylan).

As a final note on the cellulose at accessible fibril surfaces, it can be mentioned that Yoshiharu et al. [12] have recently made X-ray measurements on films of partially ordered *Cladophora* cellulose fibrils and found evidence for a rectangular cross-section in this type of fibril. The detectable difference in width of the two *Cladophora* cellulose fibril surfaces, parallel to the (1, 1, 0) and the (1, −1, 0) crystallographic planes, was slight. This may be an effect of a less-than-perfect ordering in the film of the corresponding crystallographic planes in different fibrils. Assuming that the rectangular fibril cross-sections are not artifacts due to the sample preparation procedures, qualitative information on fibril surfaces widths can be obtained. Although the observed intensity difference between the two different solvent accessible fibril surfaces, shown in Fig. 6, is large, a tentative assignment to parallel crystallographic planes would be that (1, 1, 0) and (1, −1, 0) give rise to signals at 84.5 and 83.5 ppm, respectively.

It is also interesting to note that, despite the difference in crystallinity and the dominating crystalline form of the cellulose found in *Cladophora* (triclinic cellulose Iα) and birch pulp and cotton linters [4] (monoclinic cellulose Iβ), the signals from cellulose at fibril surfaces in all celluloses appear at similar positions in the spectra. This gives an indication of the spatial distribution of the para-crystalline cellulose within the fibril immediately beneath the fibril surface, and provides a common ground for the cellulose at the fibril surface in both cellulose Iα and cellulose Iβ systems.

Table 4
The bulk average lateral dimensions of the fibrils in the different samples as determined by NMR, and some lateral fibril dimension values for similar samples reported in the literature [13] [14]

Sample	NMR fibril width (nm)	Literature values (nm)
Birch pulp	3.9 (0.2)[a]	1.5-5[b]
Cotton linters	7.1 (0.2)	7–9
Cladophora cellulose	13 (6.1)	10–35[c,d]

The NMR estimates are based on the spectra from hydrolysed samples.
[a]The values in parentheses are the standard errors.
[b]Values for *Picea abies*.
[c]Values for *Valonia*.
[d]The large error in the NMR estimate for the *Cladophora* cellulose is a result of the low signal-to-noise ratio of the surface signals.

4. Conclusion

Further experimental evidence for the spatial distribution (“in-fibril”) and the shorter relaxation time (as compared to the crystalline cellulose Iα and Iβ forms) for para-crystalline cellulose is given. A new interpretation is given for the NMR signals in the 80–86 ppm region of the spectra in terms of cellulose at (solvent) accessible fibril surfaces, cellulose at inaccessible fibril surfaces and hemicellulose (e.g., xylan). Estimates of the ^{13}C T_1-relaxation times and lateral fibril dimensions, and results from prolonged hydrolysis support this interpretation.

5. Experimental

Sample preparation.—The algal cellulose was isolated from *Cladophora* sp. naturally grown in the Baltic sea. After thorough rinsing in water it was soaked with 0.25 M HCl for 2 days at room temperature and washed with water. A procedure with repeated bleaching with $NaClO_2$ (tot. 0.2 g

$NaClO_2$/g sample) under acidic conditions at room temperature was then followed by thorough rinsing with water. The cellulose was then soaked with 0.1 M NaOH for 2 h at room temperature, washed with water to a pH of 4–5 and finally freeze dried. The wood pulp used was a bleached birch kraft pulp from a Swedish mill and the cotton linters a commercially available cotton linters (kindly supplied by Tumba Bruk AB, Sweden). Samples were subjected to hydrolysis in 2.5 M HCl at 100 °C for times between 10 min and 24 h, and then washed with water to a pH of 4–5. The ^{13}C T_1-measurement was performed on a cotton linters sample subjected to acid hydrolysis for 30 min. This sample was also used for replacement of water by methanol. About 1 g (dry weight) of wet cellulose (approximately 50% water w/w) was placed in a Pasteur pipette and eluated slowly with 40–50 mL of methanol (Merck p.a.) and was then immediately placed in an NMR sample rotor and sealed with a rotor cap.

Chemical composition.—To follow the removal of xylan, the relative proportions of the neutral polysaccharide constituents were determined by sugar analysis according to Theander and Westerlund [15]. Limiting viscosity numbers were determined according to SCAN-CM 15:88.

NMR spectroscopy.—The CP/MAS ^{13}C NMR spectra were recorded (at 292 ± 1 K) on a Bruker AMX-300 instrument operating at 7.05 T. A double air-bearing probe and a zirconium oxide rotor were used. The MAS rate was in the 4–5 kHz range. Acquisition was performed with a standard CP pulse sequence using a 3.5 μs proton 90° pulse, a 800 μs contact pulse and a 2.5 s delay between repetitions. Glycine was used for the Hartmann–Hahn matching procedure and as an external standard for the calibration of the chemical shift scale relative to tetramethylsilane [$(CH_3)_4Si$]. The data point of maximum intensity in the glycine carbonyl line was assigned a chemical shift of 176.03 ppm. The spectra were recorded on samples soaked with water or methanol. The spectra were manually phased and then normalized by setting the integrated area of each spectrum to unity. The intensities of 850 spectral points in the 55–110 ppm interval for each of the spectra were used in the principal component analysis. ^{13}C T_1-measurement was performed using a pulse-sequence developed by Torchia [16]. Six different τ-values were used: 100 μs, 1 s, 5 s, 10 s, 20 s, 40 s. Each spectrum (τ-value) was acquired using 4096 transients giving a total experiment time of 104 h. After acquisition, the C-4 region of each spectrum (τ-value) was fitted [4] and the T_1-values of the different cellulose forms were calculated based on the time dependence of the fitted signal intensities. The experiment was carried out in duplicate.

Principal component analysis, PCA.—The normalized NMR spectra of the samples were arranged in a table consisting of 19 objects (rows) and 850 variables (columns) and this table was used as input to the PCA. A number of principal components (PC) [17,18] were extracted from the mean-centered CP/MAS ^{13}C NMR data of all the samples listed in Table 2. Two statistically significant PC's were retained and these accounted for 86.8 and 10.0% of the total variance, respectively. All computations were carried out using the SIMCA-S 6.0 software package.

Acknowledgements

The study has been carried out with financial support from the Commission of the European Communities, Agriculture and Fisheries (FAIR) specific RTD program, CT96-1624. Dr. Helena Lennholm and Hoshyar Rada M.Sc. are acknowledged for their valuable contributions.

References

[1] H.A. Krässig, *Cellulose. Structure, Accessibility and Reactivity*, Polymer Monographs Vol. 11, Gordon and Breach Science, Publishers S.A., Y-Parc, Chemin de la Sallez, Yverdon, Switzerland, 1993.
[2] D.N.-S. Hon and N. Shiraishi (Eds.), *Wood and Cellulosic Chemistry*, Marcel Dekker, New York and Basel, 1991.
[3] P.T. Larsson, U. Westermark, and T. Iversen, *Carbohydr. Res.*, 278 (1995) 339–343.
[4] P.T. Larsson, K. Wickholm, and T. Iversen, *Carbohydr. Res.*, 302 (1997) 19–25.
[5] R.H. Atalla, J.C. Gast, O.W. Sindorf, V.J. Bartuska, and G.E. Maciel, *J. Am. Chem. Soc.*, 102 (1980) 3249–3251.
[6] W.L. Earl and D.L. VanderHart, *J. Am. Chem. Soc.*, 102 (1980) 3251–3252.
[7] R. Teeäär, R. Serimaa, and T. Paakkari, *Polymer Bull.*, 17 (1987) 231–237.
[8] P. Wormald, K. Wickholm, P.T. Larsson, and T. Iversen, *Cellulose*, 3 (1996) 1–12.
[9] R.H. Newman, *Holzforshung*, 52 (1998) 157–159.

[10] D.L. VanderHart and R.H. Atalla, *Further Carbon-13 NMR Evidence for the Coexistence of Two Crystalline Forms in Native Celluloses*, in R.H. Atalla (Ed.), *The Structures of Cellulose*, ACS Symp. Ser. no. 340, 88–118, American Chemical Society, Washington DC., 1987.
[11] H. Lennholm, L. Wallbäcks, and T. Iversen, *Nordic Pulp Pap. Res. J.*, 10 (1994) 46–50.
[12] N. Yoshiharu, K. Shigenori, W. Masahisa, and O. Takeshi, *Macromolecules*, 30 (1997) 6395–6397.
[13] H.F. Jakob, D. Fengel, S.E. Tschegg, and P. Fratzl, *Macromolecules*, 28 (1995) 8782–8787.
[14] H.-P. Fink, D. Hofmann, and B. Philipp, *Cellulose*, 2 (1995) 51–70.
[15] O. Theander and E.A. Westerlund. *J. Agric. Food Chem.*, 34 (1986) 330–336.
[16] D.A. Torchia, *J. Magn. Reson.*, 30 (1978) 613–616.
[17] I.T. Jolliffe, *Principal Component Analysis*, Springer-Verlag, New York, 1986.
[18] S. Wold, C. Albano, W.J. Dunn III, U. Edlund, K. Esbensen, P. Geladi, S. Hellberg, E. Johansson, W. Lindberg, and M. Sjöström, *Chemometrics. Mathematics and Statistics in Chemistry*, in B.R. Kowalski (Ed.), *Multivariate Data Analysis in Chemistry*, D. Reidel, Dordrecht, The Netherlands, 1984.